SDC-93-406

SDC
SOLENOIDAL DETECTOR NOTES

TRACK SEGMENT RECONSTRUCTION IN STRAW SUPERLAYERS

January 1993

W.T. Ford
University of Colorado

COLO – HEP – 306
SDC – 93 – 406
January, 1993

Track Segment Reconstruction in Straw Superlayers

W. T. FORD

Department of Physics, University of Colorado
Boulder, Colorado 80309-0390

As described in the SDC Technical Design Report (TDR),[1] the straw tracker is configured as five cylindrical superlayers, each containing six or eight layers of straw tube detectors in a close-packed configuration. The layout of straws and modules within the superlayers is shown in Fig. 1. The organization of the measurements into superlayers effects a substantial reduction of measurement combinations to be investigated in the track finding. The first phase of data reduction is to link hits within a superlayer into segments, resolve right/left ambiguities, and fit for local position and direction within about 85 μm and 0.01 radians, respectively. This information can be used to eliminate many fragments of loopers and to sort segments into bins related to curvature for the formation of tracks. The curvature information is independent of dip angle even in the stereo layers,[2] greatly facilitating the incorporation of these measurements during the pattern recognition.

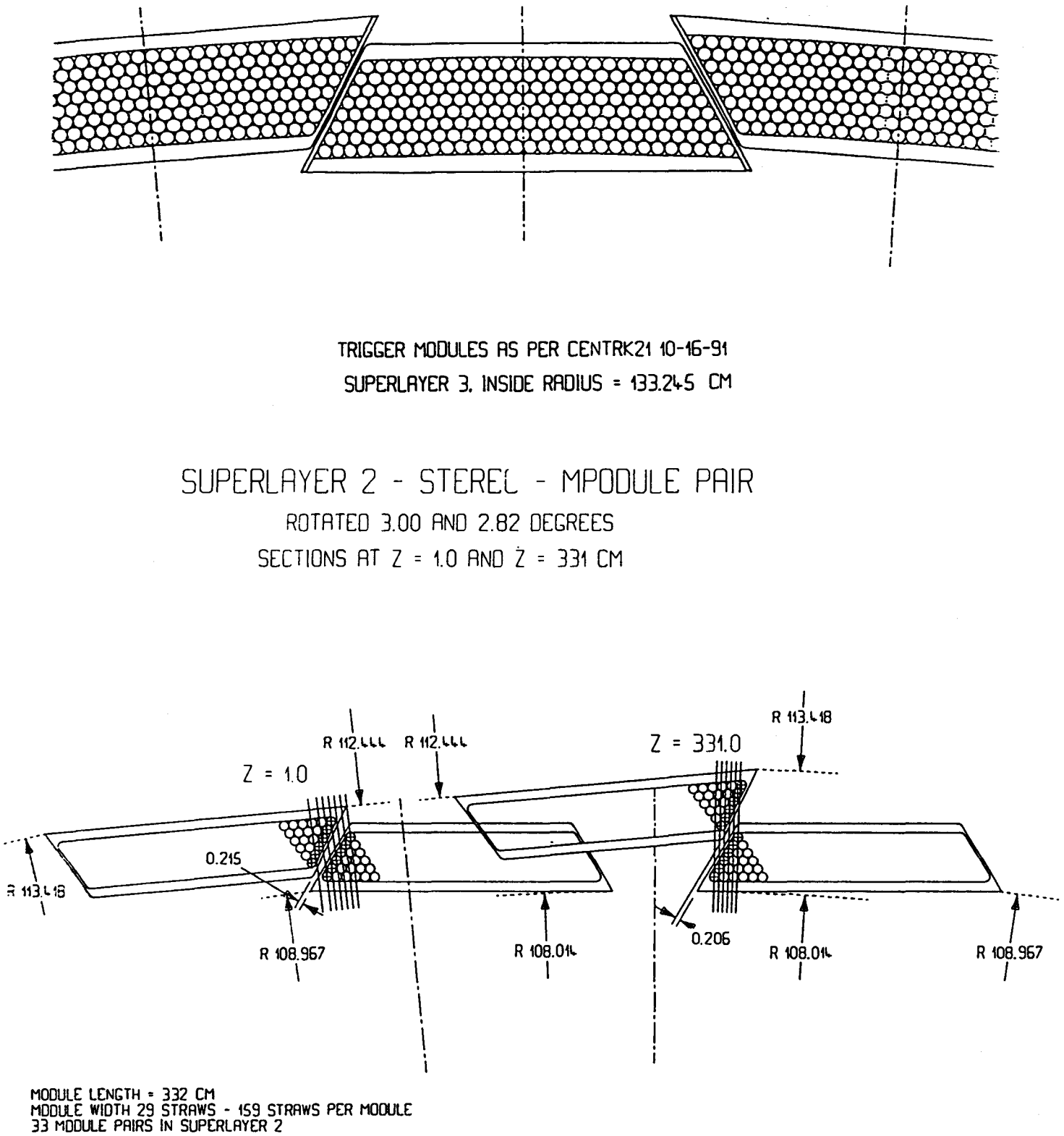

Fig. 1. Straw and module arrangement for a typical axial/trigger superlayer (above) and a stereo layer (below).

1. Simulation

The SDC tracking detector simulation allows for a detailed description of all detector elements including their inactive edges, supports, etc. The GEANT routines transport particles through the apparatus and generate decays and interactions with material, including conversions, bremsstrahlung, and delta rays. Using this program and track reconstruction algorithms we can evaluate the physics performance of the detector both at design luminosity and at higher luminosities.

With these simulation tools we have studied a number of physics processes, including the decay of a neutral Higgs boson (mass = 300 GeV) $H^0 \rightarrow Z^0 Z^0 \rightarrow e^+e^-\mu^+\mu^-$. The ISAJET generator was used to produce the Higgs event, and PYTHIA minimum bias events were added as background. The design luminosity was simulated by a Poisson-distributed mean of 1.6 background events for each bunch crossing, with a total of 7 crossings (-4 to $+2$ from the crossing with the Higgs) used to account for loopers and allow for long drift times in the straw system. The background was scaled appropriately to simulate 3 and 10 times design luminosity.

1.1. Occupancy

With a drift velocity in the straw tubes of about 70 μm/ns (with 2 T magnetic field), and a shaping time of about 25 ns, we expect an average dead time of about 40 ns.[3] A hit which occurs during the on-time of the discriminator output is not recorded, but does extend the deadtime interval. This effect is included in the simulation. Digitizations which map into valid drift distance values (with allowance for resolution) are used in the segment finder. The acceptance range corresponds to a time gate of about 40 ns. The occupancy (probability that at least one hit occurs within the time gate) is shown as a function of detector radius from the beam line in Fig. 2(a) for design luminosity. Fig. 2(b) shows the occupancy when a Higgs event is added to the minimum bias interactions at 1, 3, and 10 times

design luminosity. We find that these Higgs events produce additional occupancy equivalent to about that of mimimum bias events at design luminosity.

We note here that a rough estimate of occupancy can be made from the knowledge that pp collisions produce about 6.5 particles per unit of rapidity, given the rapidity acceptance, azimuthal size, and radial placement of the detectors. The results for superlayers 1, 3, and 5 are 3.7%, 2.4%, and 1.6%, respectively. This calculation produces an underestimate because of its neglect of the effect of bending in the magnetic field, especially in the inner superlayers, as we observe by comparing with Fig. 2.

The contribution of photons and neutrons from the material of the calorimeter is not in the simulation. It has been estimated independently.[1,4] and found to be small compared with that of particles from the interaction point.

1.2. Expected Segment Efficiency

The occupancy gives a measure of the probability to miss a hit, since the readout electronics record only one time measurement per deadtime interval. A rough estimate of the impact of deadtime on segment reconstruction efficiency can be made by evaluating the probability to get the minimum number of hits given the number of layers, with the assumption that we have an azimuthally random flux of particles through the detector (ignoring correlations).

Assume that to see a segment in a superlayer of $N_s = 6$ or 8 straw layers we need $n = 4$ hits. The probability $P(\geq n|N_s)$ is given by the binomial distribution,

$$P(\geq n|N_s) = \sum_{i=n,N_s} \frac{N_s!}{n!(N_s-n)!} p^n (1-p)^{(1-n)},$$

with p the probability to get the signal in one cell, i.e., that no background hit occur in the dead time range τ_d prior to the signal. For a Poisson distributed population $p = \exp(-R\tau_d)$. The background rate R can be inferred from the occupancy O

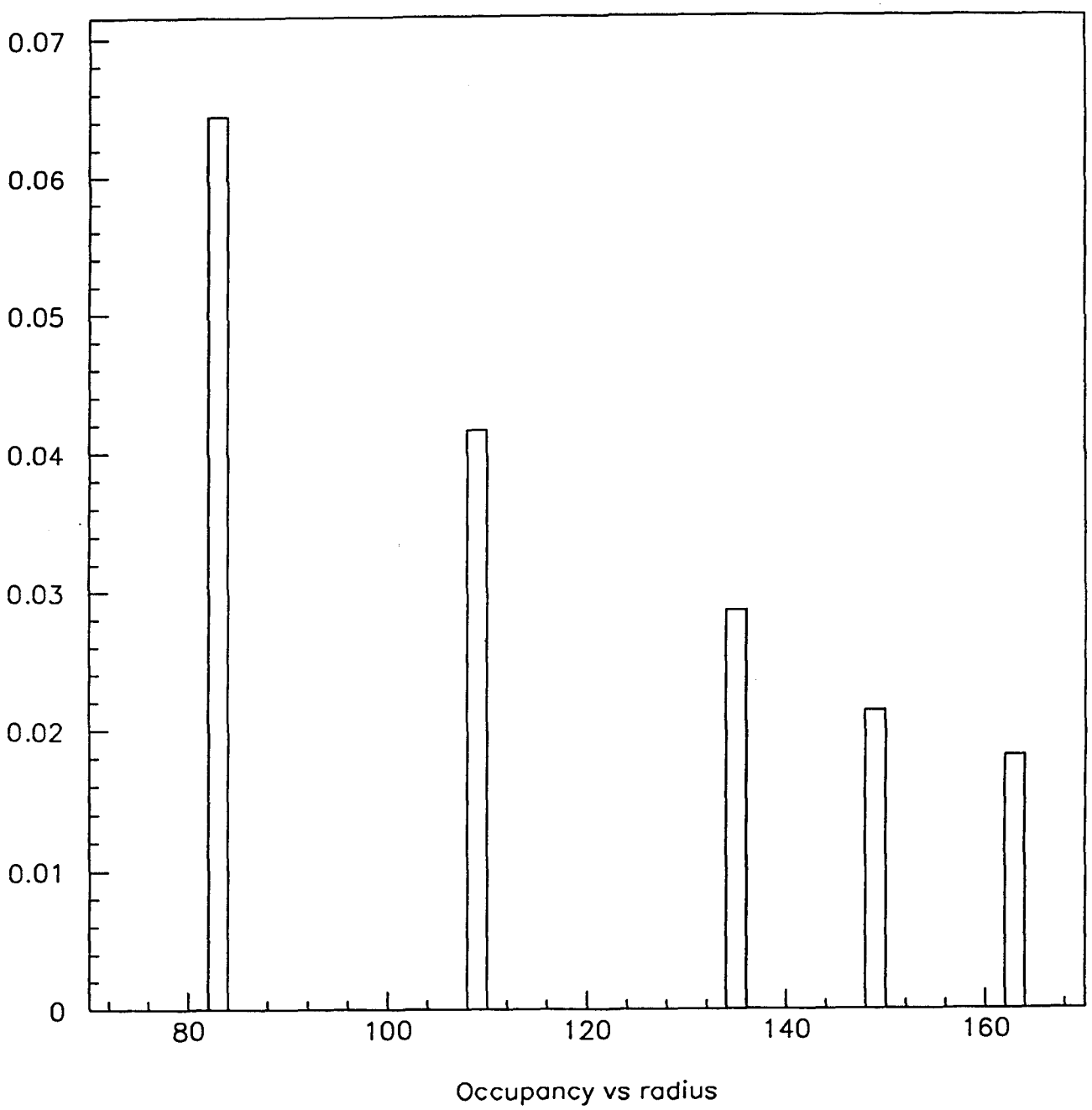

Fig. 2. (a) Occupancy at design luminosity for the five straw superlayers, as a function of the detector distance (radius) from the beam line.

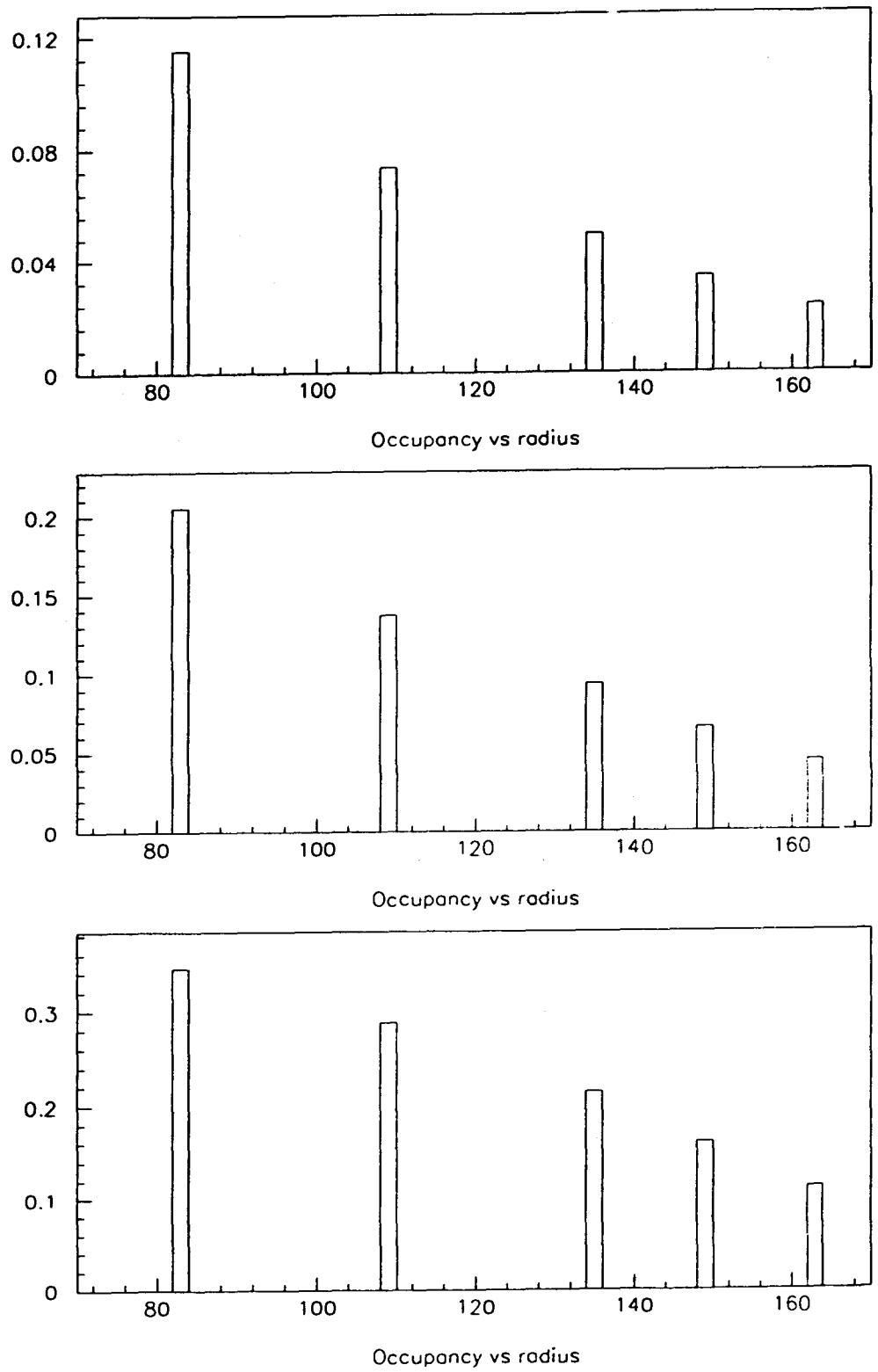

Fig. 2. (b) (Top to bottom: luminosity = 1, 3, 10 times design.) Occupancy from minimum bias interactions plus a Higgs event.

since in the acceptance gate τ_a

$$1 - O = e^{-R\tau_a},$$
$$R = -\frac{1}{\tau_a}\log(1 - O),$$
$$p = (1 - O)^{\tau_d/\tau_a}.$$

With $\tau_d = \tau_a$ (=40 ns), p is just $1-O$. The results are shown for the five superlayers as a function of luminosity in Fig. 3.

This method of estimating efficiency brings home one result that has been obscured by statistics in the simulations until recently: superlayers with eight straw layers are more efficient than ones with six. The figure shows that superlayer 2 is no better (in fact is worse at lower luminosity) than superlayer 1, even though it's at a larger radius. Similarly for the comparison of superlayers 3 and 4. It also shows that reasonable efficiencies may be achieved in the outer three straw superlayers out to 10 times design luminosity.

We note also that the probability for confusion in the pattern recognition, given that enough hits are present, is lower than for missing a hit, since the time measurement localizes the hit within about 10% of a straw radius.

1.3. Resolution

The straw Tracker CDR[5] specifies the expected intrinsic resolution (from electron diffusion in the gas, time walk, etc) of 120 microns per measurement, internal alignment of detectors within a superlayer of 30 microns, error from lack of straightness of the modules of 45 microns, and from placement of the modules of 45 microns. If we assume 90% efficiency for hits included on segments, the results of adding these in quadrature are 87 (83) microns for 6 (8) layer superlayers. In the simulations we have set the resolution to 150 μm for the segment reconstruction to approximate the combination of these effects.

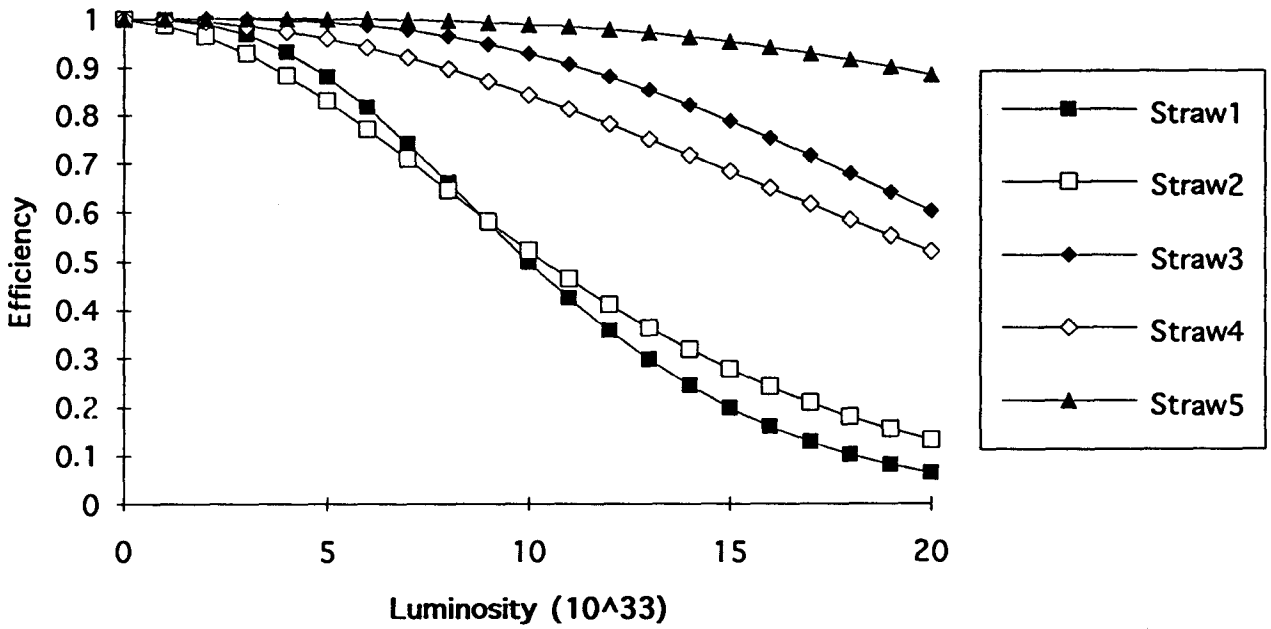

Fig. 3. Probability to get at least 4 hits in the straw superlayers as a function of luminosity, assuming no azimuthal correlations among hits.

2. Segment Reconstruction Algorithm

The time measurement can be converted into a simple circular contour of distance from the wire, to which the trajectory is tangent. This fact is not altered by the magnetic bending of the drift electron trajectory, but does assume that the arrival time of the signal at the readout electronics is given solely by the drift time. In fact the delay caused by particle time of flight to the detector and propagation of the signal pulse along the wire to its end is not completely negligible: it amounts to the time equivalent of roughly 100 microns of track displacement, comparable to the intrinsic resolution. Systematic variation of the pulse height may aggrevate this effect. Of course this delay is not random, and can be corrected for once a track is fully reconstructed and its axial position known. This information is not available, however, to the segment finder. Instead we treat the track crossing time as a parameter to be inferred from the segment fit, along with the azimuth and direction of the track. A constraint with uncertainty corresponding to the range of track arrival delays (Gaussian approximation) is included in the fit.

The segment finder works as follows: one superlayer is considered at a time. For definiteness assume it has layers numbered 1 to 8 from the interaction point outward. The outermost program loop searches layer 8, 7, 6, ... for a first hit, the starting point for a candidate segment. The next loop, nested within the first, searches layers 1, 2, 3, ... for a hit with azimuth not too different from that of the first hit. For this pair of hits we have four choices of right/left ambiguity, and each is taken as a seed for the segment. The search order maximizes the hit separation so that each seed segment has a well determined direction.

The segment is interpolated in turn to each of the layers falling between those of the seed hits. Each new layer is searched for a hit within a window of the interpolated segment (both of the new hit's ambiguity signs being considered). When one is found, a least-squares fit to the augmented list of hits is performed. If the fit passes a chi-squared test, it provides an updated set of the segment parameters incorporating the new hit, which define the road for continuation to

the next layer.

The search continues through all of the internal layers, with a chi-squared test and parameter update at each stage. When the layers and hits are exhausted, enough having been successfully linked, we review the ambiguity assignments of all internal hits, refitting and selecting the best choice according the chi squared. The candidate is then saved temporarily until all four right/left choices for the seed have been considered. Finally the (up to four) condidates are compared. The test variable is: $(\mathrm{N_{layers}} - \mathrm{N_{hits}})^2 + \chi^2/\mathrm{dof}$. The candidate with the smallest value of this test variable is accepted as a segment.

Hits on the segment are excluded from further consideration as the search for more segments proceeds. This means that not all possible combinations get considered, and errors can occur because of an unlucky choice of the search order. We compensate for this in a simple manner: the program is organized so that it can be called repeatedly with the minimum number of hits as an input argument. A loop executes searches with minimum hit levels of 8, 7, ..., forcing the program to favor segments with high numbers of hits, at some cost in computer time. The results below were obtained with an absolute minimum of four hits per segment.

One feature of the straw tracker design that is not yet in the simulation or pattern recognition code is the organization of the detectors into modules. In the simulation the wires are described as if strung from points on circles at the ends. For axial superlayers this is nearly an accurate description: as shown in Fig. 1 the modules are shaped to match the curvature (so that the trigger will work), and the gaps and offsets between modules are such that each conforms to either the inner or outer eight of ten circles, with one straw missing in each layer at the transition. For the stereo superlayers a coordinate transformation must be performed in the pattern recognition code where a segment bridges two modules, and allowance made for the z-dependent position of a hit in the neighbor module. This has been worked out in detail, though not yet coded.

3. Performance results

3.1. Efficiency

A measure of the tracking efficiency at the segment level is provided by the bar plots in Fig. 4. For each layer within each superlayer we show the number of track crossings, recorded hits, and hits incorporated into segments. The sample here is all tracks having $p_\perp \geq 2$ GeV/c that come from the primary vertex for an event from the reaction $pp \rightarrow H^0X, H^0 \rightarrow Z^0Z^0 \rightarrow e^+e^-\mu^+\mu^-$, with $M(H^0) =$ 300 GeV/c^2. The open space at the top of each bar represents the loss of hits because of deadtime. The next interval, lightly cross-hatched, represents the hits that were recorded but not properly matched to segments. The last, narrow interval above the most densely cross-hatched histograms are the hits for which the wrong right-left ambiguity sign was assigned (these predominantly have drift distance less than 400 μm).

We define a properly found segment as one for which all but zero or one hits come from one of the stiff tracks as defined in the previous paragraph. The χ^2/DoF values for the segments that meet this test are shown in Fig. 5(a), and for all segments in Fig. 5(b). The latter includes good segments from lower momentum or non-primary tracks as well as fake segments. The χ^2/DoF peak appears clean for the matched segments; at high luminosity a significant bulge for the unselected segments indicates the combinatoric background that passes the fit cuts during pattern recognition.

The efficiency is the number of segments properly found divided by the number of crossings of the superlayer by a stiff track. We display this efficiency as a function of superlayer number and luminosity in Fig. 6. We note that six-layer superlayers (2 and 4) have lower efficiency compared with a smooth curve through the 1, 3, 5 points. The efficiency is reasonably high up to three times design luminosity, and for the outer three superlayers it is reasonable at ten times design luminosity.

Comparing the number of stiff segments that leave at least four hits (not

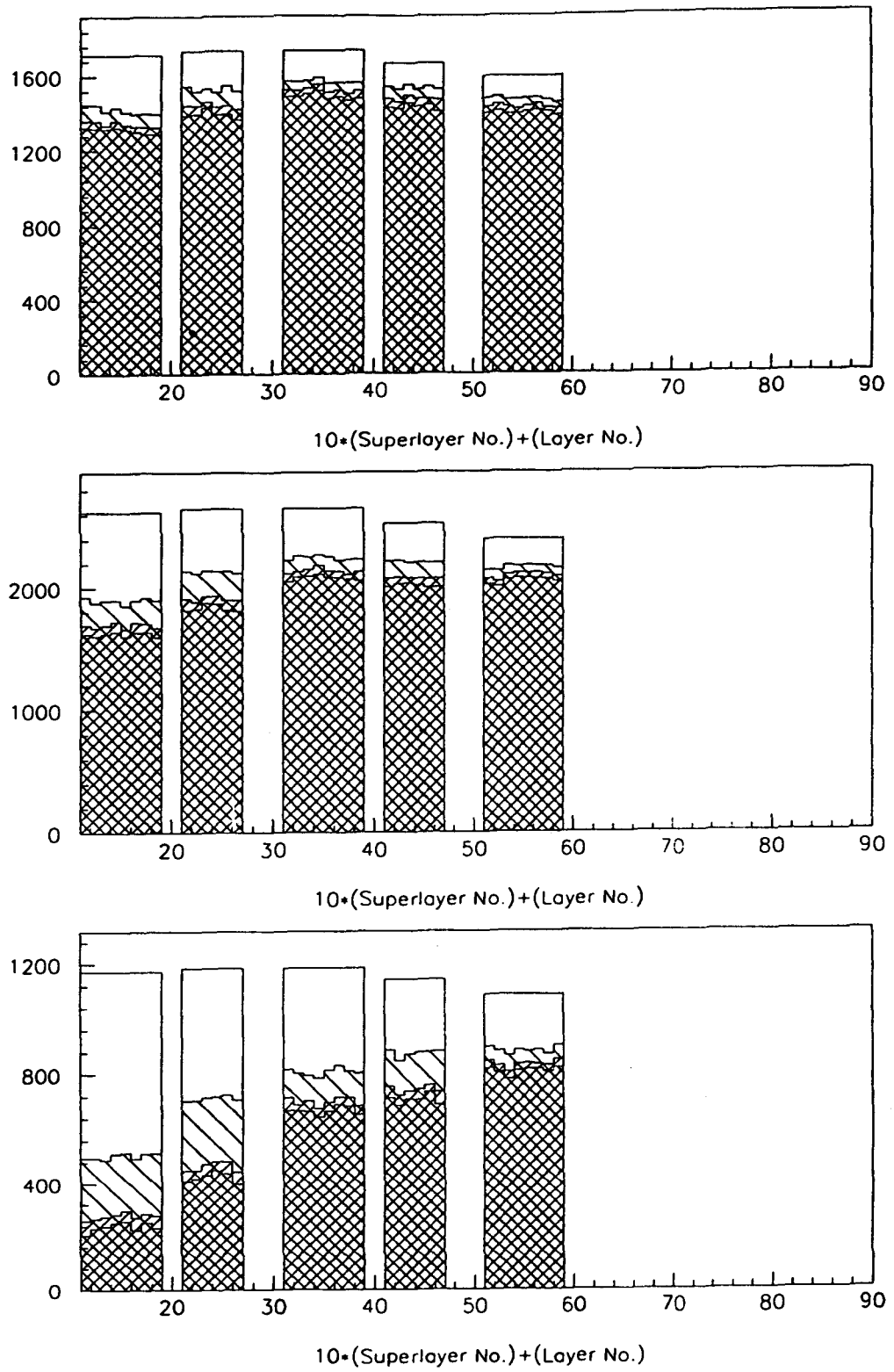

Fig. 4. (Top to bottom: luminosity = 1, 3, 10 times design.) Histograms for hits in layers of straw superlayers 1-5 (left to right): (open histogram) layer crossings by stiff track; (lightly hatched histogram) recorded digitizations; (medium hatched histogram) hits properly assigned to segments; (densely hatched histogram) hits with the proper left-right sign.

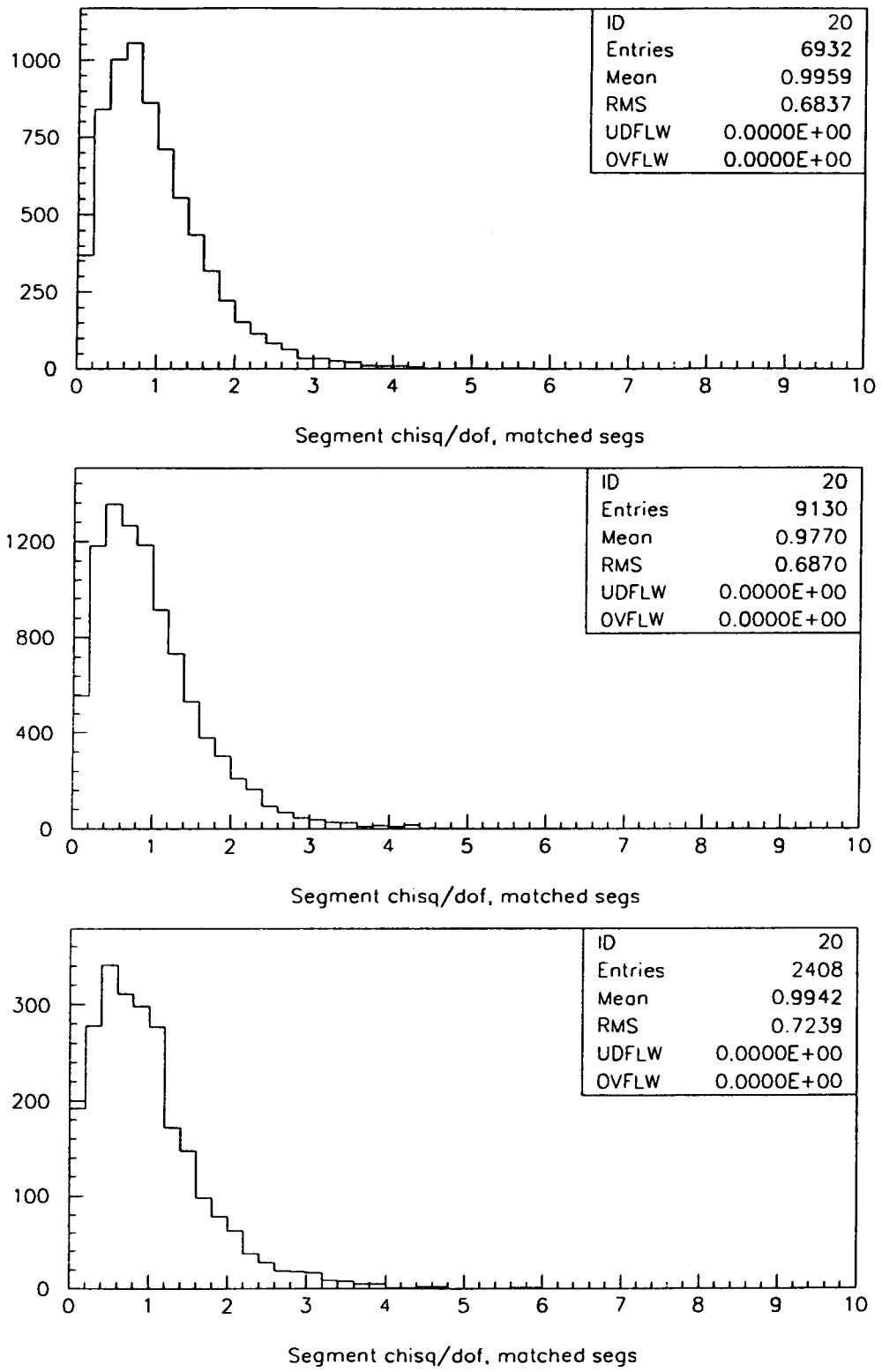

Fig. 5. (a) (Top to bottom: luminosity = 1, 3, 10 times design.) Distribution of χ^2/DoF for segments matched to stiff tracks.

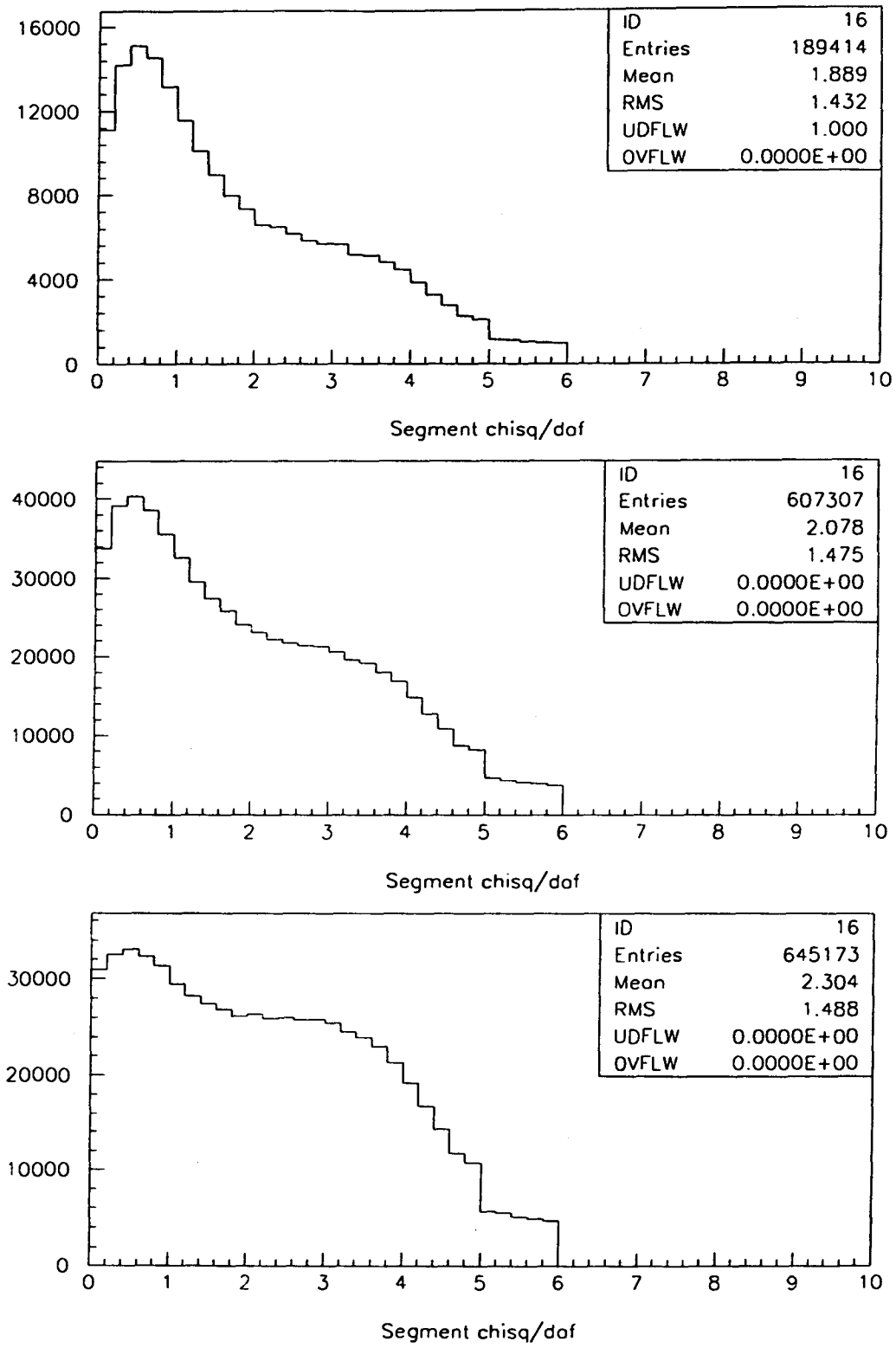

Fig. 5. (b) (Top to bottom: luminosity = 1, 3, 10 times design.) Distribution of χ^2/DoF for all segments.

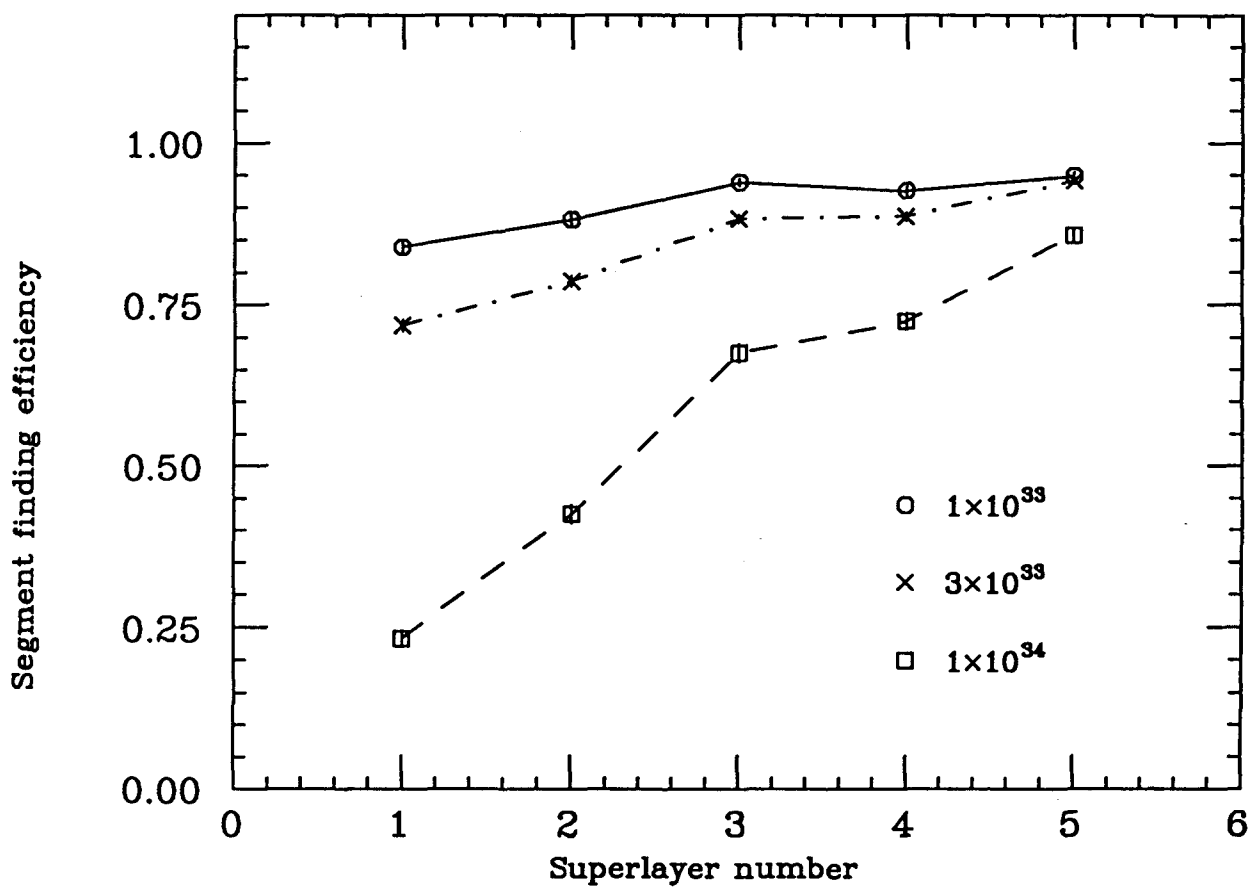

Fig. 6. Segment finding efficiency vs superlayer number for three luminosity levels as indicated.

shown) with the number that have a good segment, we find that the inefficiency attributable to the algorithm is $\lesssim 5\%$ where the efficiency is high, growing to $\sim 20\%$ where the efficiency is low (and 50% for the extreme case of superlayer 1 at 10^{34}).

3.2. Fake Segments

We measure the accuracy of segment reconstruction by finding the parent track that contributed the most hits to the segment, and then checking the number of hits from that track with the total hits on the segment. The result is shown in Fig. 7, the distribution of the fraction of hits coming from the best match track. Segments for which this fraction is high (≥ 0.75) we call real, the rest fake. (This cut is the same as the requirement of ≤ 1 wrong hit used for the stiff track efficiency, except that it accepts the case 6 right, 2 wrong. The difference in cuts is historical.) With this definition we plot in Fig. 8 the segment crossing angle for the real and fake segments. We might have expected fakes to populate large crossing angles, but this isn't what we find. At the highest luminosity there are about as many fake as real segments, compared with about 15% fake to real at design luminosity. In any case the fakes do not cause serious problems for the subsequent track finding program.

4. Conclusion

The SDC straw tracker has been modelled in considerable detail and its performance studied through simulations. Pattern recognition at the segement level is accomplished with good efficiency with low combinatoric background for luminosities well above design.

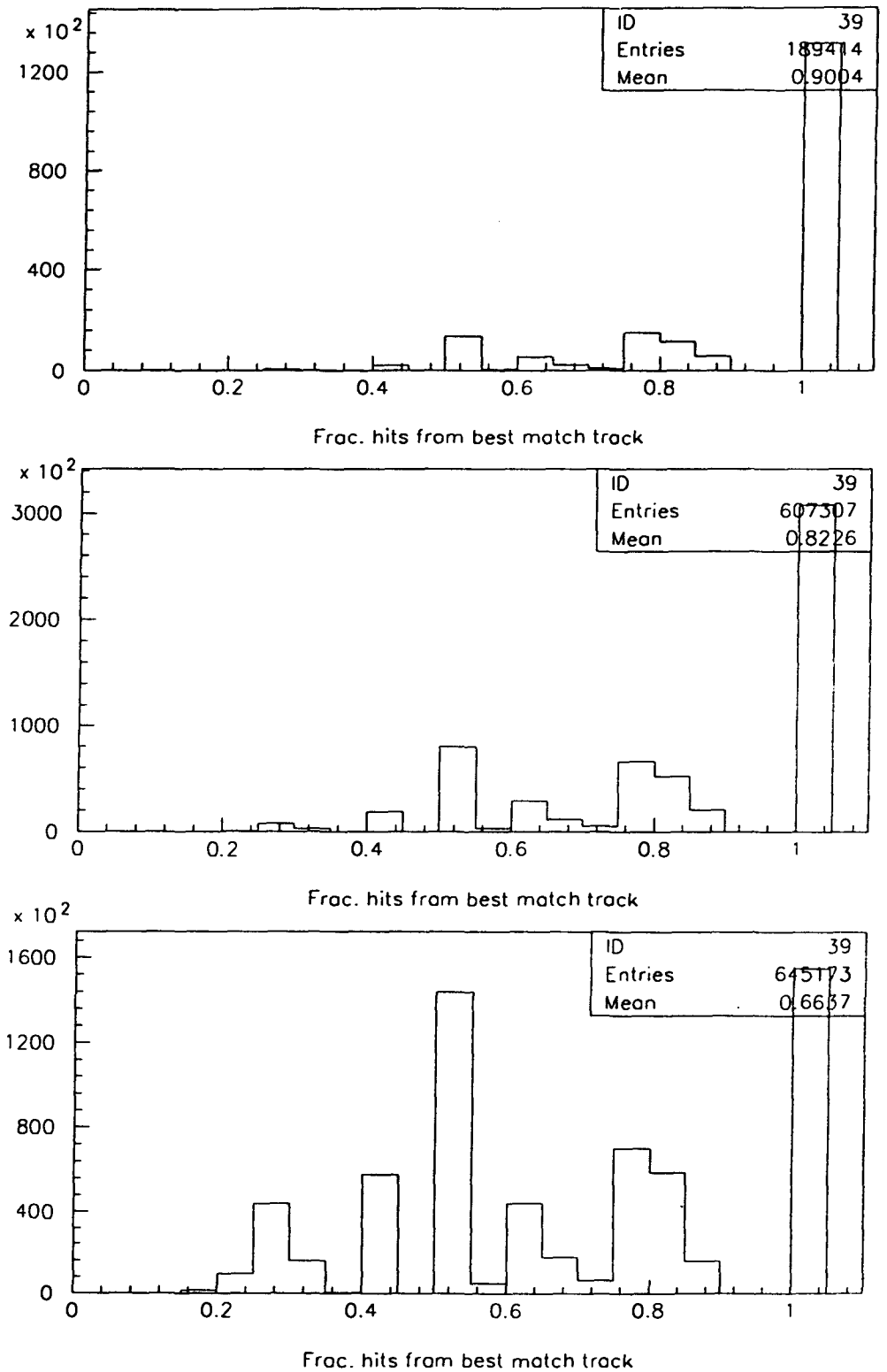

Fig. 7. (Top to bottom: luminosity = 1, 3, 10 times design.) Fraction of hits on segments coming from a common real track.

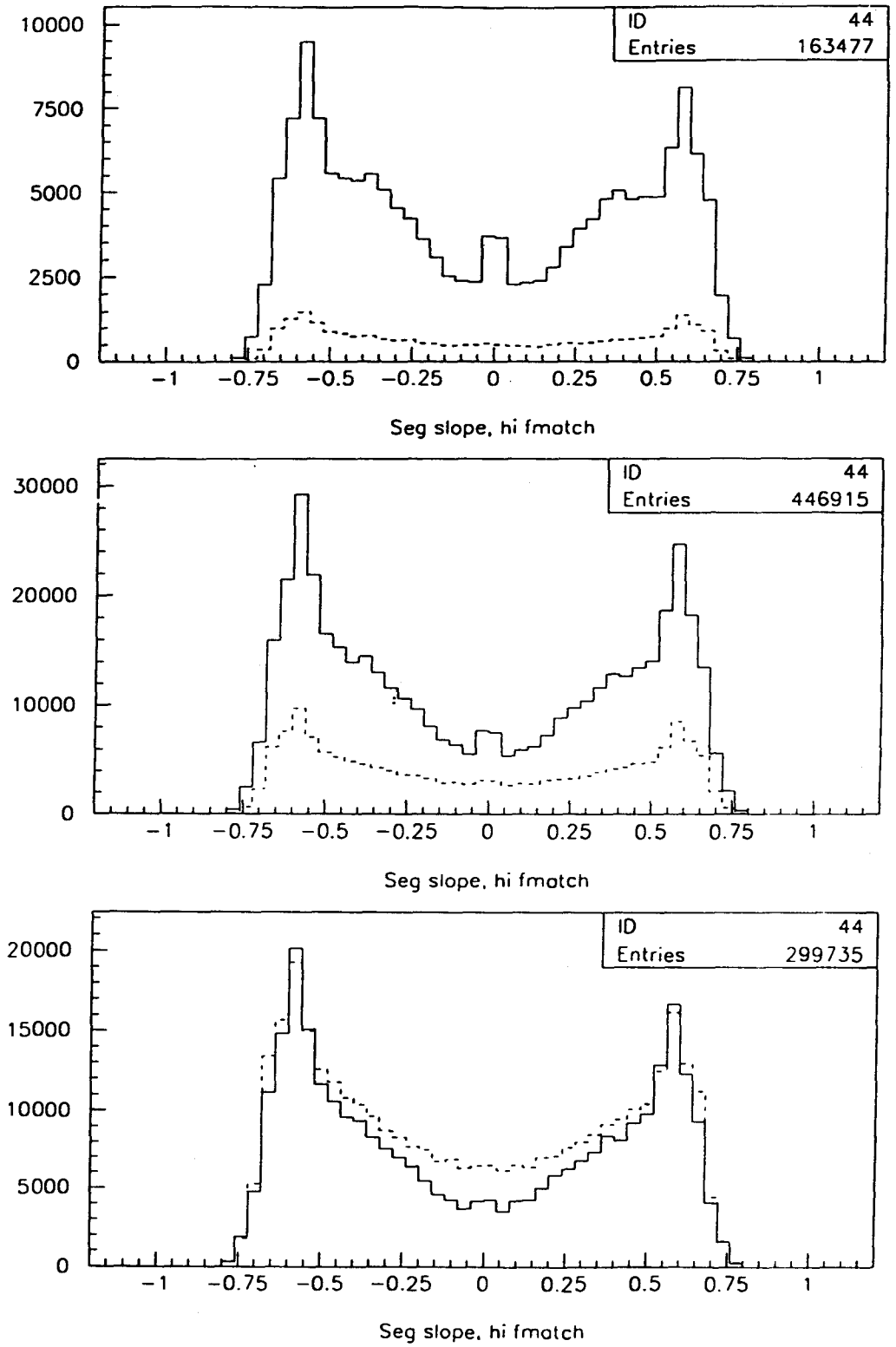

Fig. 8. (Top to bottom: luminosity = 1, 3, 10 times design.) Segment crossing angle for matched segments (solid histograms) and for fake segments (dashed histograms).

REFERENCES

1. Solenoidal Detector Collaboration, **Technical Design Report**, SDC Report SDC-92-201 (1992).
2. W. T. Ford, **Track Crossing Angle in Straw Superlayers**, SDC Report SDC-92-00227 (1992).
3. D. Craig, W. T. Ford, S. V. Greene, and M. Newcomer, SDC report (1993).
4. D. Rust, private communication.
5. SDC Straw Tracking Group, **Conceptual Design Report for the Modular Straw Outer Tracking System**, SDC Report SDC-91-00125 (1991).